International Journal of Pharmacology

ISSN 1811-7775

science alert

ansinet
Asian Network for Scientific Information

OPEN ACCESS International Journal of Pharmacology

ISSN 1811-7775
DOI: 10.3923/ijp.2024.1125.1134

Research Article
Effects of Dexmedetomidine on Proliferation, Invasion, Migration and Angiogenesis of Hypoxia-Induced HepG2 Liver Cancer Cells

[1]Di Wu, [1]Hongbao Tan, [1]Bicong Gao, [1]Xiaoyi Tang, [1]Ya Dai and [2]Yang Li

[1]Department of Anesthesiology, The Fourth Hospital of Changsha, Changsha, 410203, Hunan, China
[2]Department of Anesthesiology, The Third Hospital of Xiangya Central South University, Changsha, 410013, Hunan, China

Abstract

Background and Objective: Hepatocellular Carcinoma (HCC) is a common highly vascularized solid malignant tumor in clinical settings. This work explored the effects of dexmedetomidine (Dex) on hypoxia-induced proliferation, invasion, migration and angiogenesis of human liver cancer cells. **Materials and Methods:** The HepG2 was randomly divided into a Ctrl group (normoxic culture), a Dex group (100 μmol/L Dex under normoxic conditions), Hypoxia group (150 μmol/L $CoCl_2$ treatment) and Hypoxia+Dex group (150 μmol/L $CoCl_2$+100 μmol/L Dex treatment). Cell proliferation, cloning and migration ability, apoptosis and angiogenesis were detected using MTT assay, plate cloning, transwell assay, Hoechst 33258 staining and tubular formation assay, respectively. Western blot was used to detect the expression of Vascular Endothelial Growth Factor (VEGF) and Transforming Growth Factor-β1 (TGF-β1) protein. **Results:** It compared to the Ctrl group, the Hypoxia group showed increased proliferation activity, number of cloned and invasive cells, protein expression of VEGF and TGF-β1, decreased apoptosis rate and increased number of vascular-like structures ($p<0.05$). The behavior of cells in the Hypoxia+Dex group was opposite to that in the Hypoxia group. **Conclusion:** The Dex can inhibit the proliferation, invasion, migration and angiogenesis of HepG2 induced by hypoxia by down-regulating the expression of VEGF and TGF-1β1.

Key words: Human hepatocellular carcinoma cells, hypoxia, dexmedetomidine, proliferation, angiogenesis

Citation: Wu, D., H. Tan, B. Gao, X. Tang, Y. Dai and Y. Li, 2024. Effects of dexmedetomidine on proliferation, invasion, migration and angiogenesis of hypoxia-induced HepG2 liver cancer cells. Int. J. Pharmacol., 20: 1125-1134.

Corresponding Author: Yang Li, Department of Anesthesiology, The Third Hospital of Xiangya Central South University, Changsha, 410013, Hunan, China

Competing Interest: The authors have declared that no competing interest exists.

Data Availability: All relevant data are within the paper and its supporting information files.

INTRODUCTION

Hepatocellular Carcinoma (HCC) is a common highly vascularized solid malignant tumor in clinical settings, characterized by rapid growth. Despite its swift growth, HCC exhibits a relative lag in vascular development, resulting in an oxygen demand that surpasses microvascular oxygen supply, thereby subjecting cells within the liver cancer tissue to a prolonged state of relative hypoxia within the microenvironment[1]. Studies have confirmed that this hypoxic microenvironment induces adaptive changes in cancer cells, including stimulation of tumor angiogenesis, enhancement of anaerobic glycolysis and increased tolerance to apoptosis (Apo)[2-4]. The Hypoxia-Inducible Factor-1α (HIF-1α) plays a critical role in hypoxic response of tumors, contributing to processes such as tumor angiogenesis, resistance to radiation and chemotherapy, invasion (Inv) and metastasis[5]. Consequently, the search for effective therapeutic agents for tumors under hypoxic conditions has become a central focus of current research efforts.

Anesthetic agents can modulate the biological characteristics of residual tumor cells, inducing chemotherapy resistance and facilitating the escape of tumor cells from host defenses, thereby entering the circulatory system and giving rise to distant metastases[6]. Dexmedetomidine (Dex) is a highly selective α2 adrenergic receptor agonist, which has the functions of analgesia, sedation, anxiety relief and sympathetic response regulation. It finds wide clinical application in sedation and pain management of surgical patients[7]. The Dex is predominantly metabolized by the liver and its metabolites are excreted through urine and feces. Impaired liver function leads to a decreased clearance rate of Dex. Research has shown that Dex can activate the α2 adrenergic receptor/extracellular signal-regulated kinase signaling pathway in tumor cells, promoting breast cancer growth[8]. Nevertheless, studies by Tian *et al.*[9] indicated that Dex can inhibit ovarian cancer progression by upregulating miR-185 expression and suppressing the SOX9/Wnt/β-catenin pathway. These findings suggest that Dex exerts diverse effects on different types of tumor cells. Li *et al.*[10] analyzed the impact of Dex on oxidative stress, cell Apo, peripheral immune cells and liver function in primary liver cancer patients undergoing liver resection. The results demonstrated that Dex can mitigate oxidative stress by balancing reactive oxygen species generation and inhibiting cell Apo, thus ameliorating liver function. Nonetheless, the underlying mechanism of Dex's action on liver cancer cells remains largely unreported.

In this work, a hypoxic human HepG2 cell model was established using $CoCl_2$ and impacts of Dex on proliferation (Pro), Inv, migration (Mig) and angiogenesis of HepG2 cells following hypoxic induction were analyzed. The aim was to provide insights into the potential mechanisms of Dex in the context of tumor behavior, thereby contributing to a better understanding of its impact on tumorigenesis.

MATERIALS AND METHODS

Study area: The research was performed in The Fourth Hospital of Changsha from November, 2022 to August, 2023.

Screening of working concentration of $CoCl_2$: In the logarithmic growth phase (LGP), HepG2 cells (Wuhan Procell Life Science and Technology Co. Ltd., China) were seeded at 5×10^3 cells/well in a 96-well plate. Subsequently, distinct groups were established: The blank group (containing complete culture medium only), the Control (Ctrl) group (comprising normally cultured HepG2 cells) and the experimental group [cultured with varying concentrations of $CoCl_2$ (Guangzhou Hewei Chemical Co. Ltd., China)-supplemented medium for HepG2 cells] with each group containing 5 replicates. Following cell adherence, medium in the experimental group was replaced with a complete medium containing 0, 10, 50, 100, 150, 200, 250 and 300 μmol/L $CoCl_2$ and cells were further cultured for 24 and 48 hrs. At specific time points, 10 μL of 5 mg/mL MTT reagent was applied and incubated for 4 hrs. Subsequently, the supernatant was removed and 150 μL Dimethyl Sulfoxide (DMSO, Sigma-Aldrich Corporation, USA) reagent was applied to each well, followed by gentle mixing in the dark using a vortex mixer for 10 min. Absorbance values (A) were measured at 490 nm using SpectraMax Mini ELISA reader (Meigu Molecular Instruments Co. Ltd., Shanghai, China). For western blot (WB) analysis of HIF-1α protein expression levels (ELs), HepG2 cells were seeded at 2×10^5 cells/well. After reaching confluency, cells were cultured for an additional 48 hrs in a complete medium containing various concentrations of $CoCl_2$. Subsequently, protein ELs of HIF-1α were assessed using WB.

Cell grouping and processing: The HepG2 cells in LGP were seeded at 1×10^6 cells/well in a 6-well plate. After cell adherence, they were rolled into Ctrl, Dex, Hypoxia and the Dex-treated Hypoxia group (Hypoxia+Dex) groups. The Ctrl group was cultured conventionally without any drug treatment. In Dex group, the culture medium was

supplemented with 100 μmol/L Dex (GlpBio Inc., USA). The Hypoxia group's culture medium was supplemented with the optimal concentration of $CoCl_2$ working solution. For Hypoxia+Dex group, along with the addition of the optimal concentration of $CoCl_2$ working solution, 100 μmol/L Dex was also introduced. Following drug administration, the HepG2 cells in each group were cultured for an additional 24 hrs.

Cell pro detected by MTT assay: The HepG2 cells in the LGP were conventionally seeded. After 24 hrs of cultivation, the original culture medium was discarded and the cells were subjected to grouping treatment. According to the instructions provided with the MTT cell proliferation and cytotoxicity assay kit (Shanghai Beyotime Biotechnology Co. Ltd., China), the cells were further cultured for 12, 24, 48 and 72 hrs and 10 μL of 5 mg/mL MTT reagent was applied, followed by a 4 hrs incubation. After removing the original culture medium, 150 μL of DMSO reagent was applied and mixture was vortexed for 10 min in the dark. Subsequently, absorbance values (A) of each well were measured at 490 nm using a SpectraMax Mini ELISA reader (Meigu Molecular Instruments Co., Ltd., Shanghai, China). Cell Pro inhibition rate (PIR) was calculated (A_0 represents the absorbance of Ctrl group and A_1 represents the absorbance of Dex group or Hypoxia group or Hypoxia+Dex group):

$$\text{PIR } (\%) = \frac{A_0 - A_1}{A_0} \times 100$$

Ability of cell clone formation detected by plate cloning: The HepG2 cells in the LGP were routinely seeded. After 24 hrs of incubation, the original culture medium was discarded and the cells underwent grouping treatment. Subsequently, cells were further cultured until visible colonies formed, at which point the cultivation was terminated. The original culture medium was removed and the cells were fixed with 4% paraformaldehyde at 25°C for 30 min. Following fixation, cells were stained with crystal violet dye for 1 hr. The stained samples were then visualized under an LF200 Inverted Fluorescence Microscope (Wright Optoelectronic Technology Co. Ltd., Guangzhou, Guangdong Province, China) and five random fields were selected for the enumeration of clone cells.

Cell Inv and Mig detected by transwell: The HepG2 cells in LGP were routinely seeded. After 24 hrs incubation, the original culture medium was discarded and cells were subjected to grouping treatment. Subsequently, cells were cultured for an additional 24 hrs and then washed twice with PBS. Starvation treatment was performed by introducing serum-free DMEM and cells were incubated for 12 hrs. Cells were collected by centrifugation to prepare a single-cell suspension. Cells were then seeded in the Transwell upper chamber at 5×10^4 cells/well, while the lower chamber was supplemented with 600 μL of complete culture medium for an additional 24 hrs of incubation. Following incubation, the transwell inserts were removed and the cells not coated with Matrigel matrix gel (Corning Incorporated, USA) on the upper surface were gently wiped off using a sterile cotton swab. The remaining cells were fixed with 4% paraformaldehyde for 10 min and washed twice with phosphate-buffered saline (PBS) solution (Shanghai Yuanye Biotechnology Co. Ltd., China) before being air-dried naturally. Subsequently, cells were stained with crystal violet staining solution (Guangzhou Hewei Chemical Co. Ltd., China) staining solution for 1 hr. Stained samples were visualized under a microscope and five random fields were used for the enumeration of stained cells.

Apo morphology detected by Hoechst 33258 staining: The log-phase HepG2 cells were routinely seeded at 2.5×10^5 cells/well with glass coverslips. After 24 hrs of incubation, the original culture medium was discarded and cells were subjected to grouping treatment. Subsequently, cells were further cultured for 48 hrs and then the original culture medium was removed and the glass coverslips were retrieved. Cells were fixed with a methanol/acetic acid mixture for 5 min and then incubated at 25°C in the dark with Hoechst 33258 (Sigma-Aldrich, USA) solution after re-suspending cells. After PBS washing, cells were sealed with an anti-quenching fluorescence mounting medium. Cellular staining was observed under a LF200 Inverted Fluorescence Microscope (Wright Optoelectronic Technology Co. Ltd., Guangzhou, Guangdong Province, China), where normal cell nuclei were stained blue, while Apo cell nuclei were stained white. Five random fields were selected for Apo cell counting and Apo cell percentage was calculated using the following equation.:

$$\text{Apoptosis rate } (\%) = \frac{\text{Apoptosis cells}}{\text{Total cells}} \times 100$$

Detection of cell angiogenesis by tubule formation: Excluding the sterile packaging of ibidi angiogenesis slides, Matrigel basement membrane matrix (10 μL) was applied to each well and angiogenesis slides were incubated at 37°C for 30 min to allow gel coating. The HepG2 cells in LGP were then

routinely seeded onto the gel at 2×10^4 cells/well, followed by incubation with the corresponding culture medium for 24 hrs. Tube formation results were visualized under an LF200 Inverted Fluorescence Microscope (Wright Optoelectronic Technology Co. Ltd., Guangzhou, Guangdong Province, China) and subsequent image analysis was conducted.

EL of cell-related proteins detected by western blot (WB): The HepG2 cells in LGP were routinely seeded. After 24 hrs of incubation, the original culture medium was discarded and cells were subjected to grouping treatment. Subsequently, cells were further cultured for 48 hrs and then collected. The RIPA lysis buffer (Solarbio Corporation, USA) was applied to the cells on ice for 30 min, followed by centrifugation at 12,000 rpm for 10 min at 4°C. After the supernatant was collected, protein concentration was determined by adopting a BCA assay. The SDS-polyacrylamide gels with appropriate concentrations were prepared and proteins were separated by electrophoresis and transferred onto PVDF membranes. After blocking with a solution with 5% skim milk at 25°C for 1 hr, membranes were incubated overnight at 4°C with diluted primary antibodies including the rabbit monoclonal antibodies against HIF-1α (ab51608), VEGF (ab32152) and TGF-β1 (ab215715) and the mouse monoclonal antibody against β-actin (ab8226), all purchased from Abcam (UK), at a dilution ratio of 1:1000. Membranes were then incubated with horseradish peroxidase-conjugated secondary antibodies (ab6759, Abcam, UK) diluted at a ratio of 1:2000 at 25°C for 1 hr. Protein bands were visualized employing ECL chemiluminescence reagent (34075, Thermo Fisher, USA) and ImageJ software, integrated with a WD-9413A gel imager (Liuyi Biotechnology Co. Ltd., Beijing, China), was employed to quantify the relative grayscale values of the protein bands.

Statistical analysis: Data, denoted in Mean±Standard Deviation, were subjected to statistical analysis using SPSS 19.0. Student's t-test was employed for the comparison of differences between two independent samples, while a one-way analysis of variance was adopted for comparisons among multiple groups. The $p<0.05$ was considered statistically significant.

RESULTS

Screening of optimal concentration of the working solution of $CoCl_2$: In this work, the influence of various concentrations of $CoCl_2$ on HepG2 cell Pro was assessed using the MTT assay. In Fig. 1a, when the $CoCl_2$ concentration exceeded 200 μmol/L, the Pro activity of HepG2 cells at 24 and 48 hrs was markedly reduced versus 0 μmol/L ($p<0.05$). Nevertheless, when the $CoCl_2$ concentration was below 200 μmol/L, change in HepG2 cell pro activity at 24 and 48 hrs was not notable ($p>0.05$). The influence of different concentrations of $CoCl_2$ working solution on the protein EL of HIF-1α in HepG2 cells was assessed using the WB. In Fig. 1b, with increasing concentrations of $CoCl_2$ working solution, EL of HIF-1α protein also increased. As depicted in Fig. 1c, the HIF-1α protein EL in HepG2 cells at $CoCl_2$ concentrations exceeding 150 μmol/L was dramatically superior to at 0 μmol/L ($p<0.01$). The findings of this work indicated that when the $CoCl_2$ concentration was $\geq$150 μmol/L, both cell Pro activity and EL of HIF-1α protein undergo notable changes. Consequently, the subsequent experimental design employed a $CoCl_2$ concentration of 150 μmol/L for the induction of hypoxic cell models.

Effect of Dex on pro activity of HepG2 cells induced by hypoxia: In this work, the impact of Dex on the pro activity of hypoxia-induced HepG2 cells was assessed. In Fig. 2, the pro activity of cells in Dex group was substantially inferior to that of Ctrl group ($p<0.05$). The pro activity of cells in Hypoxia group was markedly superior to both Ctrl and Dex groups ($p<0.05$). Notably, pro activity of cells in Hypoxia+Dex group was substantially inferior to both Ctrl and Hypoxia groups ($p<0.05$).

Effect of Dex on hypoxia-induced clonal formation of HepG2 cells: How Dex impacts clonogenic potential of hypoxia-induced HepG2 cells was evaluated using a plate cloning assay. In Fig. 3a, the cloned HepG2 cells were stained purple. In Fig. 3b, number of clonogenic cells in Dex group was notably inferior to Ctrl group ($p<0.05$). Conversely, number of clonogenic cells in Hypoxia group was dramatically superior to both Ctrl and Dex groups, also exhibiting a marked difference ($p<0.05$). Similarly, number of clonogenic cells in Hypoxia+Dex group was substantially inferior to both Ctrl and Hypoxia groups ($p<0.05$).

Influence of Dex on Inv and Mig of HepG2 cells induced by hypoxia: Effects of Dex on the Inv and Mig of hypoxia-induced HepG2 cells were examined using a Transwell chamber assay. In Fig. 4a, HepG2 cells that had invaded and migrated were stained purple. As depicted in Fig. 4b, number of invasive cells in Dex group was substantially inferior to Ctrl group ($p<0.05$). Conversely, number of invasive cells in Hypoxia group was dramatically superior to both Ctrl and Dex groups ($p<0.05$). Moreover, number of invasive cells in Hypoxia+Dex group was markedly inferior to both Ctrl and Hypoxia groups ($p<0.05$).

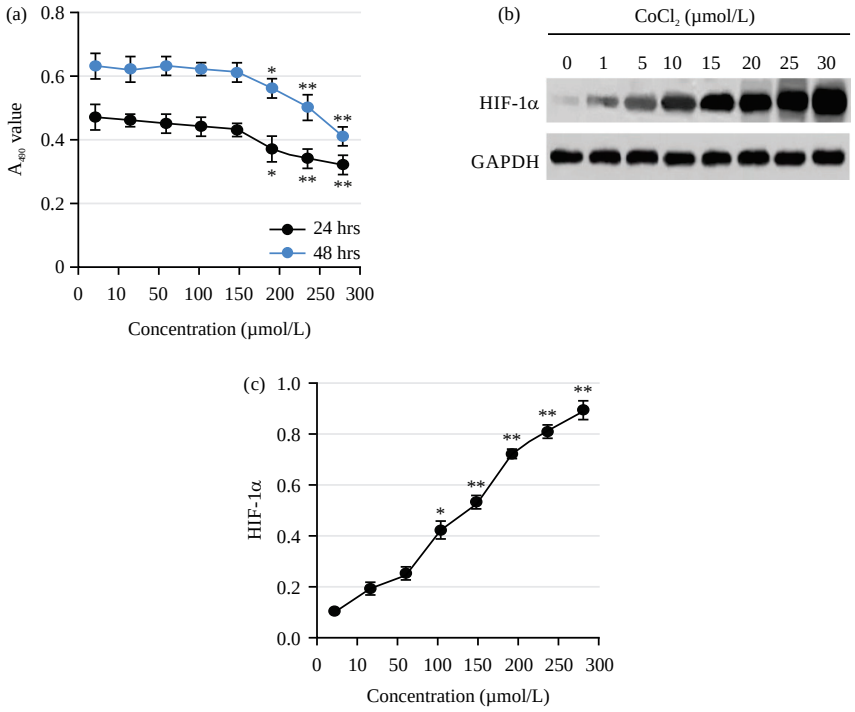

Fig. 1(a-c): Effects of various concentrations of $CoCl_2$ on HepG2 cell Pro and HIF-1α protein expression, (a) Pro of HepG2 cells detected by MTT assay, (b) EL of HIF-1α protein detected by WB and (c) Relative EL of HIF-1α protein

*p<0.05, **p<0.01 vs concentration of 0 μmol/L

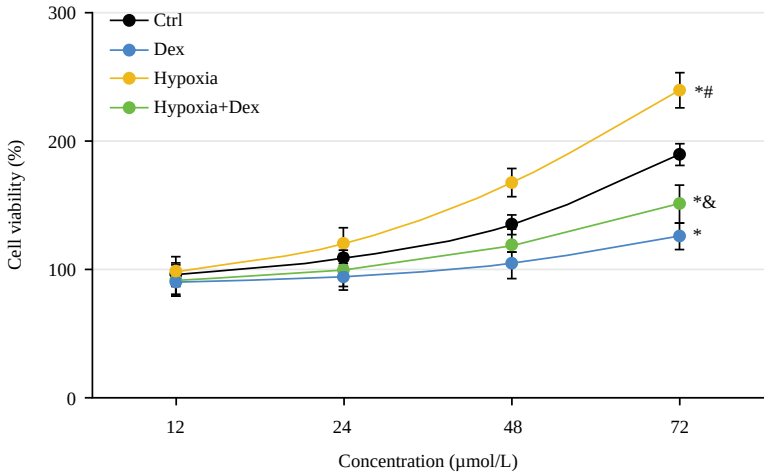

Fig. 2: Changes of Pro activity of HepG2 cells under various treatments

*p<0.05, #p<0.05 and &p<0.05 vs Ctrl, Dex and Hypoxia groups, respectively

Effect of Dex on Apo morphology of HepG2 cells induced by hypoxia: In this work, the impact of Dex on hypoxia-induced Apo in HepG2 cells was assessed using Hoechst 33258 fluorescent staining. In Fig. 5a, the number of Hoechst 33258 stained HepG2 cells in the Dex group and Hypoxia+Dex group significantly increased. In Fig. 5b, the Apo rate in Dex group was dramatically superior to Ctrl group ($p<0.05$). Conversely, the Apo rate in Hypoxia group was markedly inferior to both Ctrl and Dex groups ($p<0.05$). Furthermore, Apo rate in Hypoxia+Dex group was dramatically superior to both Ctrl and Hypoxia groups ($p<0.05$).

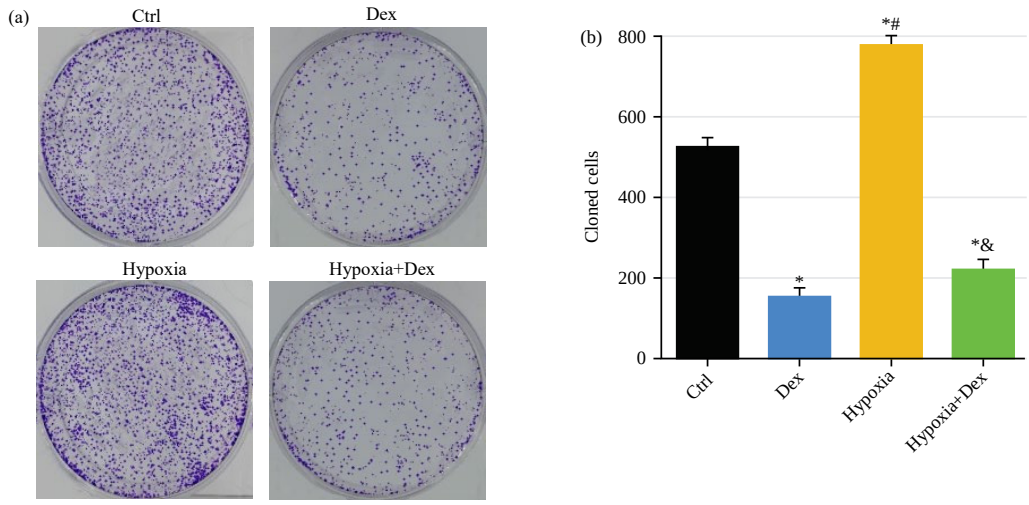

Fig. 3(a-b): Changes of clone formation ability of HepG2 cells under various treatments, (a) Cloning ability of HepG2 cells detected by plate cloning experiment and (b) Number of cloned cells
*p<0.05, #p<0.05 and &p<0.05 vs Ctrl, Dex and Hypoxia groups, respectively

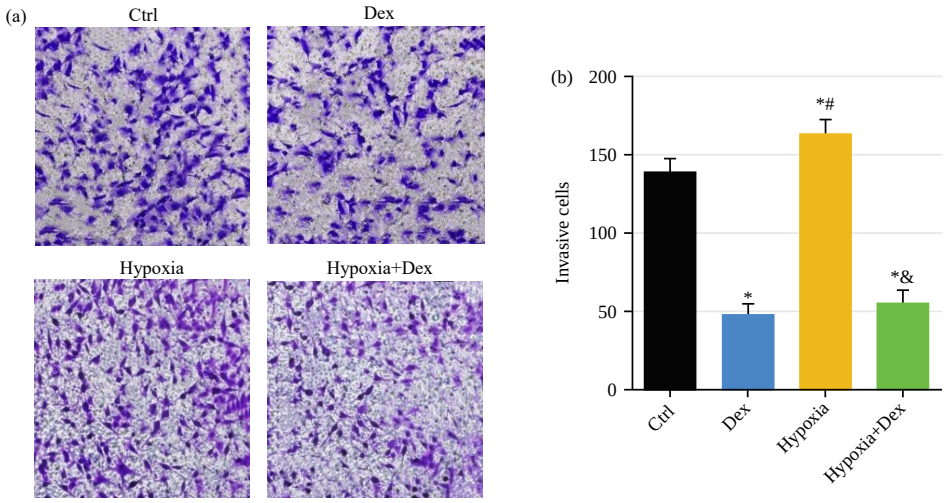

Fig. 4(a-b): Changes of Inv and Mig of HepG2 cells under different treatments, (a) Inv and Mig of HepG2 cells detected by transwell experiment (×200) and (b) Number of invasive cells
*p<0.05, #p<0.05 and &p<0.05 vs Ctrl, Dex and Hypoxia groups, respectively

Effect of Dex on angiogenesis induced by Hypoxia in HepG2 cells: In this work, the impact of Dex on the tubulogenesis ability of Hypoxia-induced HepG2 cells was observed under a microscope. In Fig. 6, the Ctrl group of HepG2 cells formed tubule-like structures, while Dex-treated HepG2 cells exhibited almost no formation of vascular-like structures. The hypoxia group demonstrated a significantly higher formation of vascular-like structures versus both the Ctrl and Dex groups. Conversely, Hypoxia+Dex group displayed notably fewer vascular-like structures than the Hypoxia group.

In this work, the impact of Dex on protein ELs of VEGF and TGF-β1 in hypoxia-induced HepG2 cells was assessed using WB analysis. In Fig. 7a is the WB detection results and there were obvious differences in the expression levels of VEGF and TGF-β1 in each group. In Fig. 7b-c, relative protein ELs of VEGF and TGF-β1 in Dex group were notably inferior to those in Ctrl group, with marked differences observed ($p<0.05$). Conversely, in Hypoxia group, relative protein ELs of VEGF and TGF-β1 were dramatically superior to those in both Ctrl and Dex groups, also implying substantial differences ($p<0.05$). Relative protein ELs of VEGF and TGF-β1 in Hypoxia+Dex group were substantially inferior to those in both Ctrl and Hypoxia groups, with considerable differences ($p<0.05$).

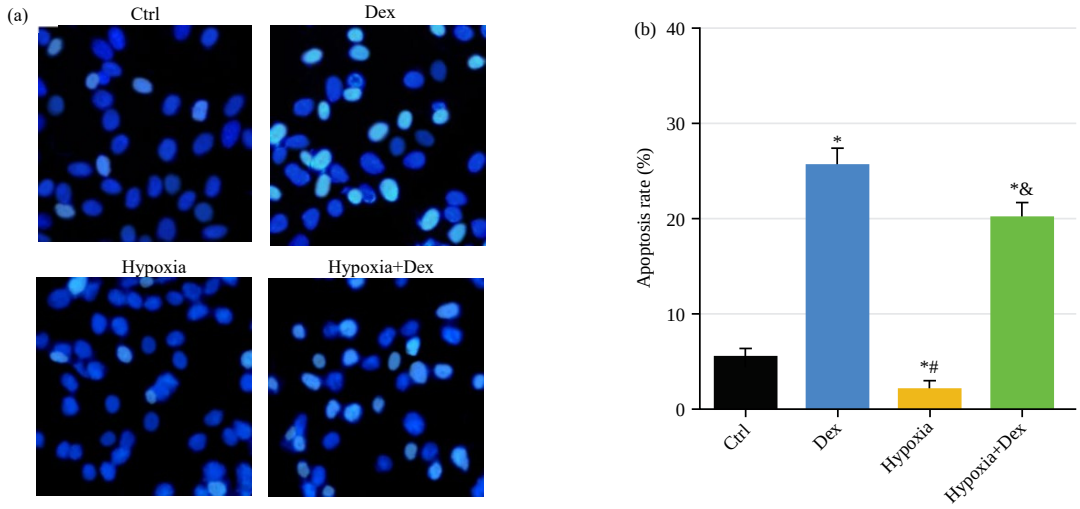

Fig. 5(a-b): Morphological changes of Apo in HepG2 cells under different treatments, (a) Hoechst 33258 staining experiment to detect HepG2 cell Apo (×200) and (b) Apo rate

*p<0.05, #p<0.05 and &p<0.05 vs Ctrl, Dex and Hypoxia groups, respectively

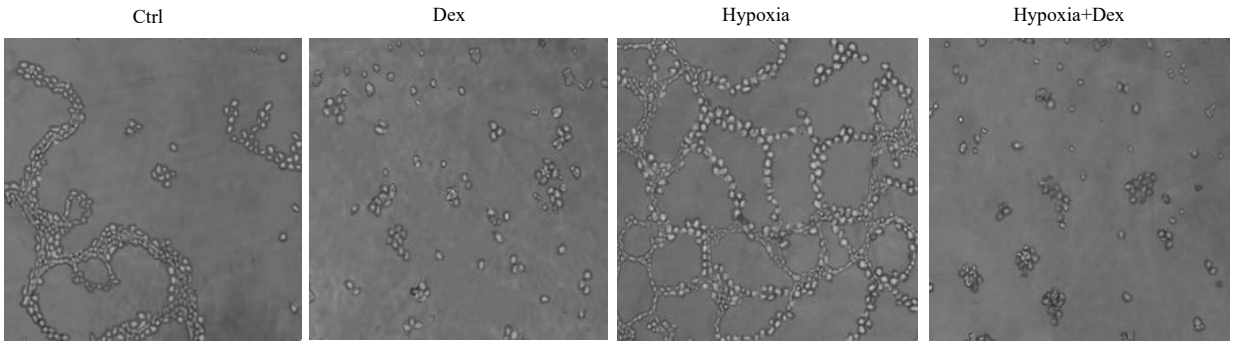

Fig. 6: Angiogenesis ability of HepG2 cells under various treatments

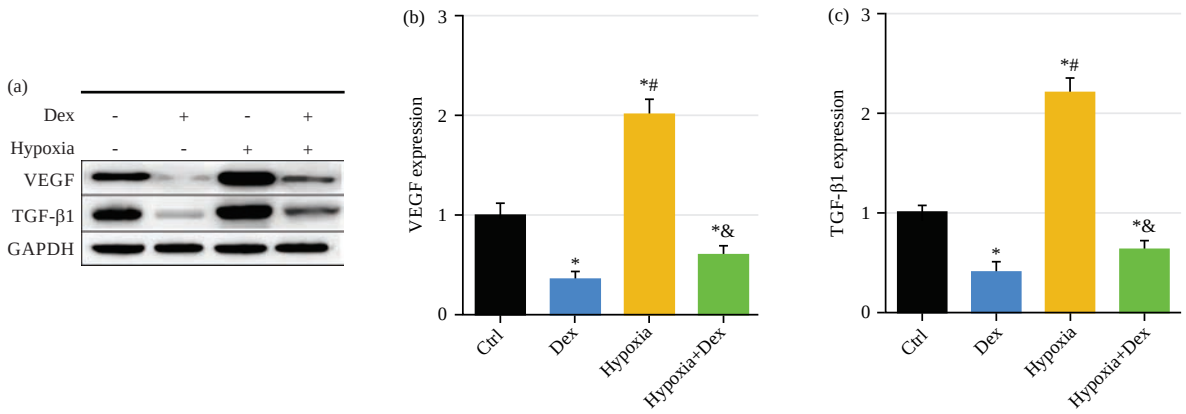

Fig. 7(a-c): Changes of VEGF and TGF-β1 protein ELs in HepG2 cells under various treatments, (a) ELs of VEGF and TGF-β1 protein detected by WB, (b) Relative EL of VEGF protein and (c) Relative EL of TGF-β1 protein

*p<0.05, #p<0.05 and &p<0.05 vs Ctrl, Dex and Hypoxia groups, respectively

DISCUSSION

The chemical induction of hypoxia, represented by $CoCl_2$, has been widely recognized by scholars. However, different types of tumor cells exhibit varying sensitivities and tolerances to $CoCl_2$, necessitating the screening of optimal concentrations[11]. The hypoxic microenvironment in tumors can induce changes in various proteins, leading to alterations in the metabolic levels of tumor cells[12]. The HIF-1α is a crucial transcription factor under hypoxic conditions, capable of promoting tumor cell proliferation, metastasis, inhibiting apoptosis and facilitating angiogenesis by activating transcriptional programs[13]. Under normoxic conditions, HIF-1α undergoes oxygen-dependent degradation, involving hydroxylation changes at specific proline residues in the oxygen-dependent degradation domain, leading to the formation of a β-folded structure in α subunit. Subsequently, it interacts with von Hippel-Lindau protein and undergoes degradation via the ubiquitin-proteasome pathway[14]. Under hypoxic conditions, this degradation pathway is inhibited, leading to the accumulation of intracellular HIF-1α, which translocates to the nucleus and forms a complex with HIF-1β, thereby initiating the transcription of downstream genes such as VEGF, participating in various physiological processes of tumor cells[15,16]. In this study, a hypoxic model of liver cancer HepG2 cells was prepared by $CoCl_2$ induction. It was observed that with increasing concentrations of $CoCl_2$, the proliferation activity of HepG2 cells gradually decreased, while the expression level of HIF-1α protein gradually increased. This indicates the successful preparation of a hypoxic HepG2 cell model.

The HCC is a highly prevalent malignant tumor characterized by rapid growth and distant metastasis[17]. The pathophysiological mechanisms underlying HCC metastasis are complex, involving the regulation of various cellular molecules, proteins and signaling pathways. The main process of HCC cell metastasis involves invading surrounding tissues, penetrating the basement membrane, entering the bloodstream, circulating to other tissues and organs and then settling and growing[18]. The hypoxic microenvironment promotes the malignancy of tumor cells and plays a significant role in inducing cancer cell drug resistance, angiogenesis and other processes[19]. Therefore, the hypoxic microenvironment is a major factor leading to the failure of chemotherapy in various solid tumors. The Dex is a commonly used anesthetic drug that can be utilized to treat persistent pain, agitation and delirium caused by tumors[20]. Additionally, studies have suggested that Dex may affect tumor spread and metastasis by enhancing capillary permeability[21]. Previous studies demonstrated that Dex exerts certain effects on the growth and metastasis of tumors such as breast cancer, lung cancer and ovarian cancer[22-24]. In this study, it was observed that the proliferation activity of HepG2 cells significantly decreased after treatment with Dex. This indicates that Dex can reverse the increased proliferation activity induced by hypoxia in HepG2 liver cancer cells. The colony formation assay is an important method used to evaluate cell proliferation, invasiveness and sensitivity to cytotoxic factors[25]. The colony formation rate reflects cell population dependence and proliferative capacity[26]. It was found in this study that after treatment with Dex under hypoxic conditions, both the colony formation ability and invasive capacity of HepG2 cells were significantly reduced. This suggests that Dex can reverse the enhanced colony formation ability and invasiveness of HepG2 liver cancer cells induced by hypoxia, thereby inhibiting cell proliferation, growth and metastasis.

The occurrence, progression, metastasis and recurrence of HCC involve multiple factors, with cellular hypoxia being implicated in the progression of HCC. The hypoxic tumor microenvironment can induce changes in various proteins, leading to metabolic alterations in tumor cells. The HIF-1 regulates multiple hypoxia-inducible genes involved in angiogenesis, tumor invasion and resistance to radiotherapy and chemotherapy[27,28]. The Dex, an α2 adrenergic receptor agonist, exerts analgesic and sedative effects. Studies have also shown that Dex plays a role in anti-inflammatory and organ protection against ischemic and hypoxic injuries[29]. In this study, it was observed that treatment of HepG2 cells with Dex under hypoxic conditions significantly increased the rate of apoptosis. Hypoxia suppresses apoptosis in liver cancer cells, while the combined application of Dex can reverse the apoptotic effect of hypoxia on cancer cells, thereby promoting apoptosis in cancer cells. Tumor angiogenesis refers to the process of growing new blood vessels from pre-existing capillary networks. Angiogenesis plays an extremely important role in the growth, metastasis and prognosis of malignant solid tumors. In a hypoxic tumor environment, the inactivation of proteins such as HIF1-α inhibition prevents the hydroxylation of HIF-1/HIF-2α, reducing the binding of HIFα to E3 ligases, promoting the entry of HIFα-HIFβ dimers into the cell nucleus, activating angiogenesis-related genes and promoting tumor angiogenesis mimicry[30-32]. Angiogenesis primarily relies on the action of pro-angiogenic factors, with Vascular Endothelial Growth Factor (VEGF) being the most specific and potent pro-angiogenic factor. Elevated levels of VEGF expression stimulate endothelial cell division and proliferation, significantly promoting neovascularization[33]. Cell factors such as TGF-β1 can induce the expression of VEGF[34].

The VEGF stimulates angiogenesis, promotes endothelial cell proliferation and migration, increases vascular permeability and facilitates the action of certain proteases to degrade the extracellular matrix, thereby contributing to tumor angiogenesis, infiltration and metastasis[35,36]. Hypoxia induction can upregulate the expression of VEGF[37]. The results confirmed that Dex can inhibit hypoxia-induced pseudo-angiogenesis in HepG2 cells and the expression levels of VEGF and TGF-β1 in cells are also significantly reduced. These findings demonstrated that Dex can inhibit the expression of VEGF and TGF-β1 in HepG2 cells induced by hypoxia, thereby suppressing neovascularization.

CONCLUSION

Treatment of HepG2 cells with 150 μmol/L $CoCl_2$ effectively established a hypoxic cell model, leading to marked inhibition of cell Pro and promotion of HIF-1α protein EL. Under hypoxic induction, HepG2 cell Pro activity was enhanced, resulting in increased numbers of clonogenic and invasive cells, reduced Apo rate, augmented pseudovascular-like formations and elevated ELs of angiogenesis-related proteins. Following Dex application under hypoxic conditions, HepG2 cell Pro activity diminished, clonogenic and cell numbers decreased, Apo rate increased, pseudovascular-like formations were inhibited and ELs of VEGF and TGF-β1 were reduced. These findings indicate that Dex can reverse hypoxia-induced Pro and Inv of HepG2 cells and suppress pseudovascular-like formation by downregulating angiogenesis-related protein expression. To further comprehend the relationship between Dex and liver cancer, along with its underlying mechanisms, the establishment of a liver cancer xenograft animal model is warranted to investigate Dex's *in vivo* distribution characteristics and its effects on inhibiting liver cancer xenograft growth and metastasis.

SIGNIFICANCE STATEMENT

Dexmedetomidine is a type of anesthetic metabolized by the liver, which has been proven to be involved in regulating the progression of some cancers, but its mechanism of action on liver cancer still needs further exploration. The purpose of this study was to explore the effect of dexmedetomidine on hypoxia induced malignant biological behavior of HepG2 cells and to find that it can significantly inhibit the proliferation, migration/invasion and angiogenesis of HepG2 cells under these conditions. This result can provide an experimental basis for further exploring the mechanism by which dexmedetomidine affects the progression of liver cancer.

REFERENCES

1. Wu, Q., W. Zhou, S. Yin, Y. Zhou and T. Chen *et al*., 2019. Blocking triggering receptor expressed on myeloid cells-1-positive tumor-associated macrophages induced by hypoxia reverses immunosuppression and anti-programmed cell death ligand 1 resistance in liver cancer. Hepatology, 70: 198-214.
2. Wicks, E.E. and G.L. Semenza, 2022. Hypoxia-inducible factors: Cancer progression and clinical translation. J. Clin. Invest., Vol. 132. 10.1172/JCI159839.
3. Korbecki, J., D. Simińska, M. Gąssowska-Dobrowolska, J. Listos, I. Gutowska, D. Chlubek and I. Baranowska-Bosiacka, 2021. Chronic and cycling hypoxia: Drivers of cancer chronic inflammation through HIF-1 and NF-κB activation: A review of the molecular mechanisms. Int. J. Mol. Sci., Vol. 22. 10.3390/ijms221910701.
4. Infantino, V., A. Santarsiero, P. Convertini, S. Todisco and V. Iacobazzi, 2021. Cancer cell metabolism in hypoxia: Role of HIF-1 as key regulator and therapeutic target. Int. J. Mol. Sci., Vol. 22. 10.3390/ijms22115703.
5. Huang, R., L. Zhang, J. Jin, Y. Zhou and H. Zhang *et al*., 2021. Bruceine D inhibits HIF-1*α*-mediated glucose metabolism in hepatocellular carcinoma by blocking ICAT/*β*-catenin interaction. Acta Pharm. Sin. B, 11: 3481-3492.
6. Piccioni, F., A. Poli, L.C. Templeton, T.W. Templeton and M. Rispoli *et al*., 2019. Anesthesia for percutaneous radiofrequency tumor ablation (PRFA): A review of current practice and techniques. Local Reg. Anesth., 12: 127-137.
7. Kaye, A.D., D.J. Chernobylsky, P. Thakur, H. Siddaiah and R.J. Kaye *et al*., 2020. Dexmedetomidine in enhanced recovery after surgery (ERAS) protocols for postoperative pain. Curr. Pain Headache Rep., Vol. 24. 10.1007/s11916-020-00853-z.
8. Liu, Y., J. Sun, T. Wu, X. Lu and Y. Du *et al*., 2019. Effects of serum from breast cancer surgery patients receiving perioperative dexmedetomidine on breast cancer cell malignancy: A prospective randomized controlled trial. Cancer Med., 8: 7603-7612.
9. Tian, H., L. Hou, Y. Xiong and Q. Cheng, 2021. Dexmedetomidine upregulates microRNA-185 to suppress ovarian cancer growth via inhibiting the SOX9/Wnt/β-catenin signaling pathway. Cell Cycle, 20: 765-780.
10. Li, W., M. Chen, Y. Gong, F. Lin and C. Sun, 2023. Effects of dexmedetomidine on oxidative stress, programmed cell death, liver function, and expression of peripheral immune cells in patients with primary liver cancer undergoing hepatectomy. Front. Physiol., Vol. 14. 10.3389/fphys.2023.1159746.
11. Rana, N.K., P. Singh and B. Koch, 2019. $CoCl_2$ simulated hypoxia induce cell proliferation and alter the expression pattern of hypoxia associated genes involved in angiogenesis and apoptosis. Biol. Res., Vol. 52. 10.1186/s40659-019-0221-z.

12. Bader, J.E., K. Voss and J.C. Rathmell, 2020. Targeting metabolism to improve the tumor microenvironment for cancer immunotherapy. Mol. Cell, 78: 1019-1033.
13. Janbandhu, V., V. Tallapragada, R. Patrick, Y. Li and D. Abeygunawardena *et al*., 2022. *Hif-1a* suppresses ROS-induced proliferation of cardiac fibroblasts following myocardial infarction. Cell Stem Cell, 29: 281-297.E12.
14. Kim, J., D. So, H.W. Shin, Y.S. Chun and J.W. Park, 2015. HIF-1α upregulation due to depletion of the free ubiquitin pool. J. Korean Med. Sci., 30: 1388-1395.
15. Tirpe, A.A., D. Gulei, S.M. Ciortea, C. Crivii and I. Berindan-Neagoe, 2019. Hypoxia: Overview on hypoxia-mediated mechanisms with a focus on the role of HIF genes. Int. J. Mol. Sci. Vol. 20. 10.3390/ijms20246140.
16. Zhang, D., F.L. Lv and G.H. Wang, 2018. Effects of HIF-1α on diabetic retinopathy angiogenesis and VEGF expression. Eur. Rev. Med. Pharmacol. Sci., 22: 5071-5076.
17. Anwanwan, D., S.K. Singh, S. Singh, V. Saikam and R. Singh, 2020. Challenges in liver cancer and possible treatment approaches. Biochim. Biophys. Acta (BBA) Rev. Cancer, Vol. 1873. 10.1016/j.bbcan.2019.188314.
18. Jin, C., P. Kumar, J. Gracia-Sancho and J.F. Dufour, 2021. Calcium transfer between endoplasmic reticulum and mitochondria in liver diseases. FEBS Lett., 595: 1411-1421.
19. Bao, M.H.R. and C.C.L. Wong, 2021. Hypoxia, metabolic reprogramming, and drug resistance in liver cancer. Cells, Vol. 10. 10.3390/cells10071715.
20. Nair, A.S., M.S. Saifuddin, V. Naik and B.K. Rayani, 2020. Dexmedetomidine in cancer surgeries: Present status and consequences with its use. Indian J. Cancer, 57: 234-238.
21. She, H., Y. Hu, Y. Zhou, L. Tan and Y. Zhu *et al*., 2021. Protective effects of dexmedetomidine on sepsis-induced vascular leakage by alleviating ferroptosis via regulating metabolic reprogramming. J. Inflammation Res., 14: 6765-6782.
22. Mohta, M., B. Kalra, A.K. Sethi and N. Kaur, 2016. Efficacy of dexmedetomidine as an adjuvant in paravertebral block in breast cancer surgery. J. Anesth., 30: 252-260.
23. Wang, C., T. Datoo, H. Zhao, L. Wu and A. Date *et al*., 2018. Midazolam and dexmedetomidine affect neuroglioma and lung carcinoma cell biology *in vitro* and *in vivo*. Anesthesiology, 129: 1000-1014.
24. Shin, S., K.J. Kim, H.J. Hwang, S. Noh, J.E. Oh and Y.C. Yoo, 2021. Immunomodulatory effects of perioperative dexmedetomidine in ovarian cancer: An *in vitro* and xenograft mouse model study. Front. Oncol., Vol. 11. 10.3389/fonc.2021.722743.
25. Wang, B., B.S. He, X.L. Ruan, J. Zhu and R. Hu *et al*., 2022. An integrated microfluidics platform with high-throughput single-cell cloning array and concentration gradient generator for efficient cancer drug effect screening. Mil. Med. Res., Vol. 9. 10.1186/s40779-022-00409-9.
26. Tristan, C.A., H. Hong, Y. Jethmalani, Y. Chen and C. Weber *et al*., 2023. Efficient and safe single-cell cloning of human pluripotent stem cells using the CEPT cocktail. Nat. Protoc., 18: 58-80.
27. Manuelli, V., C. Pecorari, G. Filomeni and E. Zito, 2022. Regulation of redox signaling in HIF-1-dependent tumor angiogenesis. FEBS J., 289: 5413-5425.
28. Wang, Y., X. Wei, Y. Jiao, Y. Bai and S.W. Noel *et al*., 2022. STAT3/HIF-1α/fascin-1 axis promotes RAFLSs migration and invasion ability under hypoxia. Mol. Immunol., 142: 83-94.
29. Cai, S., Y. Liu, Y. Cheng, J. Yuan and J. Fang, 2022. Dexmedetomidine protects cardiomyocytes against hypoxia/reoxygenation injury via multiple mechanisms. Clin. Lab. Anal., Vol. 36. 10.1002/jcla.24119.
30. Ai, X., P. Yu, L. Luo, J. Sun, H. Tao, X. Wang and X. Meng, 2022. *Berberis dictyophylla* F. inhibits angiogenesis and apoptosis of diabetic retinopathy via suppressing HIF-1α/VEGF/DLL-4/Notch-1 pathway. J. Ethnopharmacol., Vol. 296. 10.1016/j.jep.2022.115453.
31. de Heer, E.C., M. Jalving and A.L. Harris, 2020. HIFs, angiogenesis, and metabolism: Elusive enemies in breast cancer. J. Clin. Invest., 130: 5074-5087.
32. Bartoszewski, R., A. Moszyńska, M. Serocki, A. Cabaj and A. Polten *et al*., 2019. Primary endothelial cell-specific regulation of hypoxia-inducible factor (HIF)-1 and HIF-2 and their target gene expression profiles during hypoxia. FASEB J., 33: 7929-7941.
33. Pulkkinen, H.H., M. Kiema, J.P. Lappalainen, A. Toropainen and M. Beter *et al*., 2021. BMP6/TAZ-Hippo signaling modulates angiogenesis and endothelial cell response to VEGF. Angiogenesis, 24: 129-144.
34. Scola, L., M.R. Bongiorno, G.I. Forte, A. Aiello and G. Accardi *et al*., 2022. *TGF-β/VEGF-A* genetic variants interplay in genetic susceptibility to non-melanocytic skin cancer. Genes, Vol. 13. 10.3390/genes13071235.
35. Ahir, B.K., H.H. Engelhard and S.S. Lakka, 2020. Tumor development and angiogenesis in adult brain tumor: Glioblastoma. Mol. Neurobiol., 57: 2461-2478.
36. Vimalraj, S., 2022. A concise review of VEGF, PDGF, FGF, Notch, angiopoietin, and HGF signalling in tumor angiogenesis with a focus on alternative approaches and future directions. Int. J. Biol. Macromol., 221: 1428-1438.
37. Florentin, J., S.P. O'Neil, L.L. Ohayon, Afaz Uddin and S.B. Vasamsetti *et al*., 2022. VEGF receptor 1 promotes hypoxia-induced hematopoietic progenitor proliferation and differentiation. Front. Immunol., Vol. 13. 10.3389/fimmu.2022.882484.